Methoxy radical adsorption on gold nanoparticles: a comparison with methanethiol and methylamine radicals

Xavier Fenouillet, Magali Benoit, Nathalie Tarrat

Noname manuscript No.
(will be inserted by the editor)

Methoxy radical adsorption on gold nanoparticles - A comparison with methanethiol and methylamine radicals

Xavier Fenouillet · Magali Benoit · Nathalie Tarrat*

Received: date / Accepted: date

Abstract The adsorption of a methoxy radical (OCH_3) on the low-energy flat gold surfaces Au(111), Au(100) and Au(110) and on surface defects (adatoms) was compared with those of methanethiol (SCH_3) and methylamine ($NHCH_3$) radicals. Using dispersion-corrected DFT, we showed that the adsorption energy of OCH_3 on gold is significantly lower than that of SCH_3 but not very far from that of $NHCH_3$. Whatever the molecule, we found that the adsorption energy is of the same order on Au(110) and Au(100), and smaller on Au(111) and that the charge transfer goes from the surface to the molecule. The charge transferred to SCH_3 is very small, while that transferred to $NHCH_3$ is slightly larger, but still three times smaller than in the case of OCH_3. Concerning the competition between adsorption sites, we observed that undercoordinated atoms are not systematically more favoured than flat surfaces.

Keywords Gold Nanoparticles · Methoxy · Methanethiol · Methylamine · Adsorption

1 Introduction

Due to their biocompatibility, gold nanoparticles (AuNPs) are increasingly studied for biomedical applications such as biosensing, cancer treatment, bacterial control, imaging, diagnosis, detection and drug delivery [1,2]. For most of these applications, the AuNPs surfaces are functionalized with organic ligands. In most cases, these latter are grafted on the AuNPs through a sulfur atom, and to a lesser extent, through a nitrogen atom [3,4]. Unraveling the grafting modes of these ligands makes it possible to design more stable functionalized AuNPs with increased efficiency and, in some cases, to limit off-target toxicity [3]. A much less attention is paid to the functionalization of AuNPs through oxygen atoms. Indeed, articles can be found in the literature describing the use of polyvinyl alcohol as a stabilizer [5] but none, to our knowledge, describing a R-O group as functional ligand grafted on an AuNP. The interaction between R-O ligands and a gold surface has therefore been much less studied than that of amines and thiols, from both experimental and theoretical points of view. To contribute to the filling of this gap, we have implemented numerical simulations to quantify the difference in adsorption on AuNPs (energetics and structure) between a methoxy radical OCH_3, and the corresponding thiol and amine radicals, SCH_3 and $NHCH_3$. This study, focused on radicals adsorption, will provide valuable information on adsorption geometries. Indeed, on a metallic substrate, the adsorption structures of radicals are similar to those of the corresponding neutral species $HOCH_3$, $HSCH_3$ and NH_2CH_3, which would have been deprotonated before arriving on the surface or once adsorbed on it. Concerning energetics, although radical species are much less stable than their hydrogenated counterparts and their probability of spontaneous generation is very low, this preliminary study allows a comparison of the adsorption energies of the methoxy and methylamine radicals with those of the methanethiol radical. To achieve a more complete picture of the adsorption paths of these three groups on gold surfaces, the next step will consist in studying the complete adsorption-deprotonation reaction paths of the neutral species. This aspect goes beyond the scope of this paper and will be the subject of a future study.

CEMES, Université de Toulouse, CNRS, 29, rue Jeanne Marvig, 31055 Toulouse, France
Tel.: +33-567524347
E-mail: nathalie.tarrat@cemes.fr

Most of the studies concerning the adsorption of our model molecules on gold are theoretical ones. Indeed, the adsorption of thiols with very short alkyl chains has been very under-explored experimentally [6–11], as well as the one of methylamine [12,13]. Concerning the adsorption of OCH_3, one can mention one experimental study focused on methanol adsorption on gold [14]. From a theoretical point of view, these systems have given rise to more investigations, but most of the time limited to the adsorption on Au(111). A large number of DFT studies have investigated the adsorption of SCH_3 or $(SCH_3)_2$ and the deprotonation of $SHCH_3$ on Au(111) [9,15–20]. According to these studies, the adsorption of the molecule on a top site (T) is less favorable than on the other studied sites, *i.e.* bridge (Br), bridge shifted to the fcc (Br_{fcc}) or to the hcp position (Br_{hcp}) and hollow sites (H_{fcc} and H_{hcp}). Adsorption of SCH_3 on undercoordinated atoms was also investigated [21–24]. In these studies, a CH_3S-Au-SCH_3 arrangement is suggested, in agreement with XSW measurements [25].

The theoretical literature describing the adsorption of thiols on surfaces other than (111) is very limited. As far as gold is concerned, one can only mention three studies [15,26,27]. For Au(100), no surface reconstruction is observed and the four-fold hollow site is found to be the most stable. For Au(110), a surface reconstruction leading to a missing row structure is described, on which the bridge/edge adsorption site is preferred. Beyond these studies, different groups have studied the thiol adsorption modes on small gold clusters[28–30]. Recent simulations have explored SCH_3 adsorption modes on a Au_{55} cluster and showed a clear preference for Br sites [31].

Computational studies focused on the adsorption of amines on gold surfaces are sparse. Liu *et al.* found the Br site as the most favourable for NH_2 adsorption, in competition with the H_{fcc} site [32]. Iori *et al.* [33] have determined the T position as the most favorable adsorption site of a histidine molecule. A comparison of the adsorption modes of the phenylamine and phenylthiolate molecules shows that, where a thiolated molecule adsorbs with very similar energy on a flat surface or with adatoms, the phenylamine molecule clearly prefers an unrebuilt surface [34]. The preferential order of amine adsorption on Au(111) sites , T > Br = H_{fcc} = H_{hcp}, was reported and this regardless the functional group carried by the nitrogen atom (hydrogen atom, methyl, phenyl, naphthyl, or anthracenyl) [35]. In this study, the adsorption is found to be systematically higher on an adatom, in contradiction with the previously mentioned study. Finally, a study addresses on protonated molecules the issue raised in the present one on radicals [36]. Indeed, the authors compare methylamine (NH_2CH_3) adsorption on Au(111) to that of methanol ($OHCH_3$) and methanethiol ($SHCH_3$) and investigate the effect of steps. They conclude that the adsorption energy of methylamine is larger than that of methanethiol and methanol, that these three molecules adsorb with the heteroatom localized on the T site and that the adsorption of methylamine is more favorable on steps. However, van der Waals forces were not taken into account in this study, even for quite large alkyl chains. A DFT comparison of the adsorption of an ethylamine molecule (CH_3-CH_2-NH_2) on clean Au(111), Au(110) and Au(100) can be found in Ref. [37]. Authors report structures in which the nitrogen atom adsorbs systematically on the T site and comparable adsorption energies are found on Au(110) and Au(100) surfaces, much higher than that observed on Au(111).

Numerical simulation studies dealing with the adsorption of the methoxy OCH_3 group on gold are also rare. Apart from the above discussed study of Lewoczko *et al.* [36], which focuses on the methanol $OHCH_3$ molecule and concludes that it has the smallest adsorption energy and the greatest distance from the gold surface when compared with methylamine and methanethiol, two other studies can be mentioned. In the first one, simulations of methoxy adsorption on transition metal surfaces describe the most favorable adsorption site as the H_{fcc} one on Au(111) [38]. In the second study, focused on methanol deprotonation on Au(100) and Au(310) surfaces, the authors determine the Br position as the most favorable one for methoxy radical [39]. In the present paper, we will compare the structures and adsorption energies on gold of a methoxy radical with those of methanethiol and methylamine radicals by studying both adsorption on flat surfaces and on surface defects (gold adatoms). In the first part of the paper, a description of our models is given together with computational details. In a second part, a structural analysis is conducted on the obtained adsorbates, these latter being ranked as a function of their adsorption energies. Charge transfers are also analyzed. In a last part, the adsorption characteristics of methoxy vs methanethiol and methylamine radicals are summarized and the adsorption on adatoms *vs* on flat surfaces is discussed. Finally, the conclusion is presented.

2 Methodology

In order to be able to study without *a priori* the nature of the interaction between a molecule and an AuNP surface, it is necessary to implement simulations in which the electronic structure is explicitly taken into account.

With this in mind, we have chosen to carry out DFT-based electronic structure calculations [40,41]. Such calculations allow a precise description of chemical interactions but the number of atoms contained in the simulated system is greatly limited by the computational cost. It is therefore impossible to simulate, using DFT, functionalized nanoparticles whose diameter is representative of those used in biomedical applications. We must use models that allow us to study the interactions between the molecules and the AuNP. To this end, we use periodic methods to simulate infinite surfaces using a simulation cell of reasonable size. This latter is periodic both in the directions parallel (x and y axes) and perpendicular (z axis) to the surface. Along the z-axis, the interactions between the molecule and the gold slab of the top periodic image are avoided by introducing a vacuum region of at least 18 Å. Along the x and y axes, the size of the box is chosen large enough so that the molecules located in two adjacent periodic boxes are separated by at least 12 Å in these two directions. The thin film used to simulate the gold surface contains 5 gold layers, the two lowest layers being kept fixed and all other atoms (three gold layers + the molecule) being allowed to relax unconstrained. The choice of the studied surfaces is based on the crystallographic facets that have the highest probability of being exposed at the surface of nanoparticles. In the case of gold, we are therefore studying the adsorption of molecules on the surfaces of low miller index (111), (100) and (110), the high stability of these three facets being attributed to their high density of atomic packing.

The DFT-based electronic structure calculations have been performed using the periodic boundary conditions VASP code [42–44] with PAW pseudopotentials [45,46]. The k-points grid was optimized for each box size. A plane wave kinetic energy cutoff of 400 eV was used (leading to an accuracy of 0.5 meV/atom) and the atomic positions were relaxed until the forces reached a value lower than 0.02 eV.Å^{-1}. For dealing with the partial occupancies around the Fermi level, a Methfessel-Paxton smearing was used with $\sigma = 0.01$ eV [47]. For evaluating electron transfers, Bader charge analysis were performed on electron density outputs from VASP [48–50]. Concerning the DFT functional chosen to conduct this study, we used a dispersion-corrected functional, optB86b-vdw [6], belonging to the vdw-DF family, developed by Dion *et al.* In this latter, the van der Waals interaction is directly obtained from the electron density by adding a non-local term to the local correlation functional. The good performance of this functional for describing gold bulk and surfaces has been validated in references [51, 52]. The use of a dispersion-corrected functional for such small adsorbates is justified by the work of Vargal *et al.* [19], who have shown that it is necessary to take these interactions into account, even for the short chains. Indeed, these authors stipulated that dispersion interactions need to be adopted to get closer to the experimental data in terms of relative height of the sulfur atom of SCH_3 over the surface.

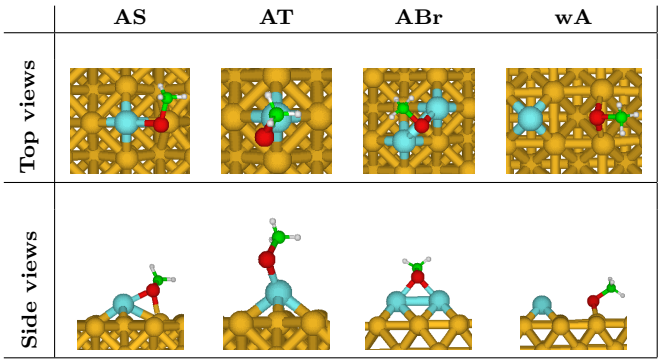

Fig. 1 Adsorption positions in presence of adatoms (gold in yellow, gold adatoms in cyan, heteroatom in red, carbon in green and hydrogen in white).

The adsorption energy of a molecule on a gold surface is calculated as :

$$E_{ads} = E_{tot} - E_{surf}^{relaxed-box} - E_{mol}^{relaxed-vacuum} \quad (1)$$

with E_{tot} being the energy of the system containing the gold slab and the molecule in the periodic cell, $E_{surf}^{relaxed-box}$ the energy of the relaxed gold slab without the molecule, and $E_{mol}^{relaxed-vacuum}$ the energy of the most stable configuration of the molecule in vacuum. A systematic study was carried out by testing all possible positions for the SCH_3, OCH_3 and $NHCH_3$ radicals on the unreconstructed Au(111), Au(110) and Au(100) surfaces: top (T), bridge (Br), longbridge (Br_l) and shortbridge (Br_s) sites on Au(110), the four-fold hollow sites (H) on Au(100) and Au(110) and the three-fold hollow sites (H_{fcc} and H_{hcp}) on Au(111). In addition, the adsorption was also investigated in the presence of one or two adatoms located on hollow sites whatever the facet. In Fig. 1 are depicted the four different studied positions of a molecule adsorbed in presence of adatoms : the heteroatom bridging an adatom and a surface atom (AS), the heteroatom on top of an adatom (AT), the heteroatom bridging two adatoms (ABr) and the molecule adsorbed on the surface far from the adatom (wA).

It should be noted that the influence of the methyl group orientation has been studied in the case of SCH_3 and the corresponding adsorption energy variations were found to be negligible. Based on this result, we decided not to explore the adsorption of rotamers of OCH_3 and $NHCH_3$. For the sake of clarity, the results corresponding to SCH_3 rotamers are not detailed.

3 Results and discussion

The adsorption energies corresponding to the adsorbates localized during our systematic exploration are gathered in Table 1. Note that all the positions explored are not necessarily stable for the 3 molecules on the 3 surfaces. In the following paragraphs, we analyze these results on a per molecule basis.

Surf	N_{ad}	Position	E_{ads} [eV]		
			SCH_3	$NHCH_3$	OCH_3
111	0	T	-1.923	-1.327	-1.402
	0	Br	-	-1.763/-1.746	-1.593
	0	Br_{fcc}	-2.315	-	-
	0	Br_{hcp}	-2.276	-	-
	0	H_{fcc}	**-2.341**	-	-1.812
	0	H_{hcp}	-2.107	-	-1.641
	1	AT (h_{fcc}*)	-2.209	-1.812	**-1.819**
	1	AT (h_{hcp}*)	-2.167	-1.763	**-1.819**
	1	AS (h_{fcc}*)	-2.270	**-1.963**	-1.484
100	0	T	-	-	-
	0	Br	**-2.718**	**-2.199**	**-1.962**
	0	H	-2.464	-	-
	1	AT	-2.105	-1.662	-1.667
	1	AS	-2.584	-2.068	-1.818
	2	ABr	-2.708	-2.138	-1.916
	1	wA-Br	-2.683	-2.180	-1.930
110	0	T	-	-	-
	0	Br_l	-2.600	-1.941	-1.783
	0	Br_s	**-2.744**	-2.163	-1.940
	0	H	-	-	-
	1	AT	-2.074	-1.685	-1.653
	1	AS	-2.717	**-2.176**	**-1.942**

Table 1 Adsorption energies of the SCH_3, $NHCH_3$ and OCH_3 radicals on Au(111), Au(100) and Au(110), according to their adsorption position. N_{ad} is the number of adatoms in the simulation cell. * h_{fcc} and h_{hcp} corresponds to the adatom position on Au(111). Numbers in bold are the most stable positions.

Adsorption of SCH_3 - On the flat Au(111) surface, the most stable adsorption sites for SCH_3 is H_{fcc}, followed by the Br_{fcc} site (+26 meV) and the Br_{fcc} one (+65 meV). These results are consistent with the previous theoretical results, these three sites being described as the most stable and very competitive with each other [9,15–18]. Regarding the comparison with experimental results, one can only mention that the bridge position has been reported in Ref. [9]. In the presence of adatoms, the preferred site on Au(111) is the AS one. On the Au(100) surface, the adsorption site that we have located as the most stable in the absence of surface defects is the Br site, in disagreement the most favorable four-fold hollow site reported in Ref[15]. However, in this study, the hollow and bridge adsorption sites are found to be energetically close (difference of 15 meV) and the DFT functional used does not take into account the dispersion forces. In the presence of adatoms, the most favorable adsorption sites are found to be the ABr and the wA-Br (+25 meV) ones. On the flat Au(110) surface, we have determined the Br_s site as the most stable one and in the presence of adatoms, the preferential adsorption site is AS, in agreement with the literature [15]. For the 3 facets, the adsorption of SCH_3 is more favourable on the flat surface than on an adatom. However, the differences vary from 71 meV for Au(111) to 8 and 27 meV for Au(100) and Au(110), respectively.

Adsorption of $NHCH_3$ - On the flat Au(111) surface, the most stable adsorption site is the Br one, consistently with the literature (only the adsorption on the top and bridge sites were found to be stable in the present study). Indeed, the Br site is described as the most favourable one for the adsorption of NH_2 [32]. In the presence of adatoms, the preferred site on Au(111) is the AS one. On Au(100), only the adsorption on a Br site is found to be stable. In the presence of one or two adatoms, two sites are competitive : the wA and the ABr (+42 meV). On Au(110), we have determined the Br_s site as the most stable with respect to the adsorption of $NHCH_3$ and the AS one in presence of an adatom. On the Au(111) surface, the adsorption on the surface with adatom is more favorable than on the flat one (+200 meV). On Au(100) and Au(110) they are competitive with a difference of 19 meV in favor of the adsorption on the flat surface for Au(100) and of 13 meV in favor of the adsorption on an adatom for Au(110).

Adsorption of OCH_3 - On the flat Au(111) surface, the most stable adsorption site is the H_{fcc} site for OCH_3, in agreement with the study reported in Ref. [38]. When adatoms are present on the surface, the most favorable sites are the AT ones (whether the adatom is in positon hollow-fcc or hollow-hcp). On Au(100), the only stable position is found to be the Br one on the flat surface in agreement with Ref. [39]. In the presence of adatoms, the wA site is the most stable, closely followed by the ABr one (+14 meV). On Au(110), we have determined Br_s as the most stable site. On this surface, the only information we have concerns the Cu(110) surface for which the Br_s site has been described as the preferential adsorption position of methoxy [53]. In the presence of adatoms, the preferential adsorption site is the AS one. On the Au(111) and Au(110) surfaces, the adsorption on the flat surface is very competitive with the one on an adatom, although the most stable position is always the one on an adatom (difference of 7 meV for Au(111) and 2 meV for Au(110)). On Au(100), the adsorption

on the flat surface is slightly favoured by 32 meV.
If we analyze these data in terms of the hierarchy of surfaces with respect to adsorption, we observe an identical overall trend, whatever the molecule, with an adsorption of the same order on Au(110) and Au(100) and less favorable on Au(111) (see Fig. 2).

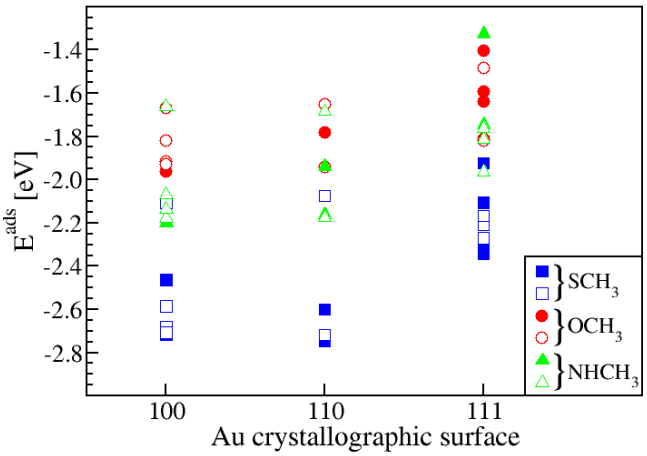

Fig. 2 Adsorption energy E_{ads} (in eV) of SCH_3 (blue), OCH_3 (red) and $NHCH_3$ (green) radicals as a function of the gold crystallographic surface Au(100), Au(110) or Au(111). Adsorptions on flat surfaces are represented by solid symbols and those involving adatoms by empty symbols.

The structural parameters of the molecules vary very little with adsorption. There is no variation in C-H bonds and the equilibrium distance of the X-C bond (X being the heteroatom) elongates during adsorption but varies very little from one adsorption site to another. It remains in the ranges : 1.822-1.835 Å for SCH_3 (with an equilibrium distance in vacuum $d_{eq-vac}^{S-CH_3}$ of 1.788 Å), 1.408-1.439 Å for OCH_3 ($d_{eq-vac}^{O-CH_3} = 1.357$ Å) and 1.450-1.476 Å for OCH_3 ($d_{eq-vac}^{HN-CH_3} = 1.436$ Å).
Selected distances describing their adsorption on gold are depicted in Fig. 3 which shows the variation of the average distance $<d_{X-Au}>$ between the heteroatom of the adsorbed molecule and its nearest gold neighbors (only gold atoms far from the heteroatom of less than 3 Å were taken into account) as a function of the distance $<d_{X-Surf}>$ between the heteroatom and the gold surface (the adsorptions on flat surfaces being represented by solid symbols and those involving adatoms by empty ones). By simulating the adsorption of the 3 molecules on an isolated gold atom, we were able to establish the reference equilibrium distances Au-X(H)CH_3 : $d_{eq-vac}^{Au-SCH_3} = 2.235$ Å, $d_{eq-vac}^{Au-OCH_3} = 1.976$ Å and $d_{eq-vac}^{Au-NHCH_3} = 2.003$ Å. As expected, the $<d_{X-Au}>$ distances are systematically larger than these reference values when the molecules are deposited on the gold surfaces, and follow the ordering $<d_{S-Au}> >> <d_{O-Au}> \geq <d_{N-Au}>$. Indeed one can note that the oxygen atom of OCH_3 is a little further away from gold than the nitrogen atom of $NHCH_3$ when deposited on the surface. For the 3 molecules, the X-Au distances are shorter when the adsorption is located on an adatom, whereas the average distance between the gold surface and the heteroatoms $<d_{X-surf}>$ is obviously larger when the adsorption occurs on an adatom, ranging from about 1.5 to more than 4 Å. On a flat surface, this distance lies between 1.3 and 2 Å, whatever the molecule, except in cases where the adsorption takes place on top of a gold atom. In this case, the distance is slightly larger (between 2.1 and 2.4 Å). A notable point is that, with regard to $<d_{X-Au}>$ and $<d_{X-Surf}>$, OCH_3 and $HNCH_3$ have very similar characteristics.

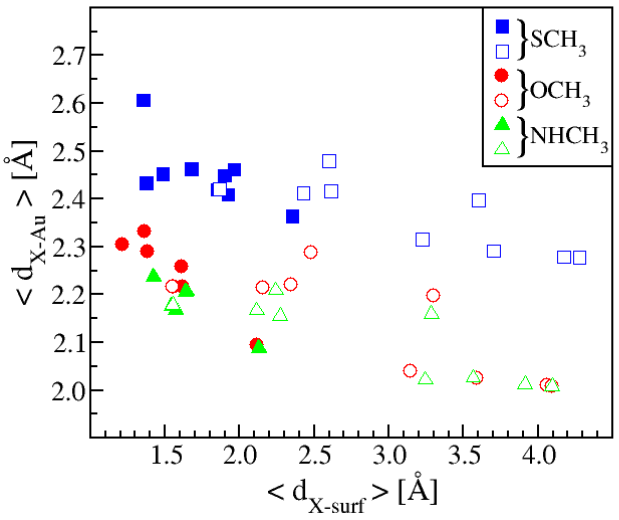

Fig. 3 Average distance $<d_{X-Au}>$ (in Å) between the heteroatom of the adsorbed radical and its nearest gold neighbors as a function of the distance $<d_{X-Surf}>$ (in Å) between the heteroatom of the adsorbed radical and the gold surface for SCH_3 (blue), OCH_3 (red) and $NHCH_3$ (green). Adsorptions on flat surfaces are represented by solid symbols and those involving adatoms by empty symbols.

The variation with $<d_{X-Surf}>$ of the tilt angle between the gold surface and the line containing the heteroatom and the carbon atom of the adsorbed molecules is depicted in Fig. 4. The tilt values are generally always lower than 50^o except for a few points corresponding to the five adsorptions in a hollow position localized on

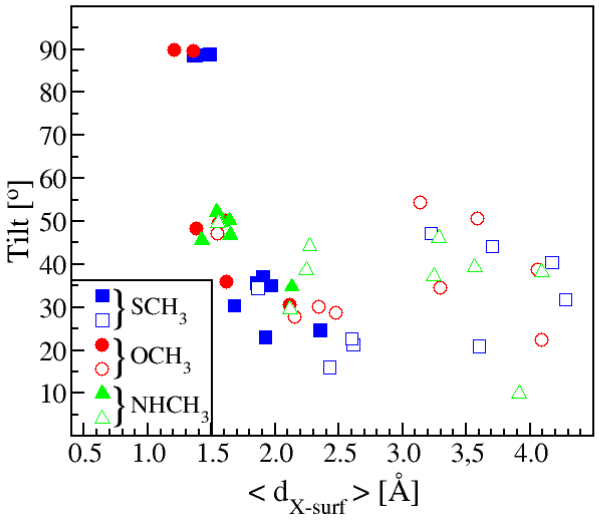

Fig. 4 Tilt angle (in °) between the gold surface and the line containing the carbon atom and the heteroatom of the adsorbed SCH_3 (blue), OCH_3 (red) and $NHCH_3$ (green) radicals as a function of the average distance $<d_{X-Surf}>$ (in Å) between the heteroatom of the adsorbed radical and the gold surface. Adsorptions on flat surfaces are represented by solid symbols and those involving adatoms by empty symbols.

the flat surfaces (see Table 1), for which the sulphur or oxygen atom sinks into the hollow position, leading to structures where the X-C bond is perpendicular to the gold surface. On surfaces without defects, the tilt angle for SCH_3 is lower than the one of OCH_3 and $NHCH_3$, this being most likely due to longer equilibrium distances, thus allowing the molecule to position itself with a very small tilt angle with respect to the surface. The cloud of points corresponding to adsorption on adatoms is very diffuse. It should be noted, however, that tilt values remain low, due to the dispersive forces that promote greater proximity between CH_3 and the surface. For each molecule, the range of adopted tilt values is much larger when adsorption is done on an adatom. This is due to the fact that molecules can optimize their orientations in environments with lower steric encumbrances.

The variation of the adsorption energy as a function of the charge carried by the molecules is shown in Fig. 5. Whatever the molecule, the charge transfer goes from the surface to the molecule, with a much larger charge transferred in the case of OCH_3. The charge transferred to methanethiol is very small, while that transferred to methylamine is slightly larger, but still three times smaller than in the case of methoxy. In the case of SCH_3 and $NHCH_3$, the fact that the molecule adsorbs to a defectless surface or to an adatom does not seem to have any effect on the amount of electrons transferred. On the other hand, in the case of OCH_3, the transferred charge is larger when the molecule adsorbs on the surface without defects. The transferred charge seems to be molecule dependent and not related to the adsorption energy for a given molecule because the range of adsorption energies corresponding to charge transfers of similar amplitude is very extended for the 3 molecules.

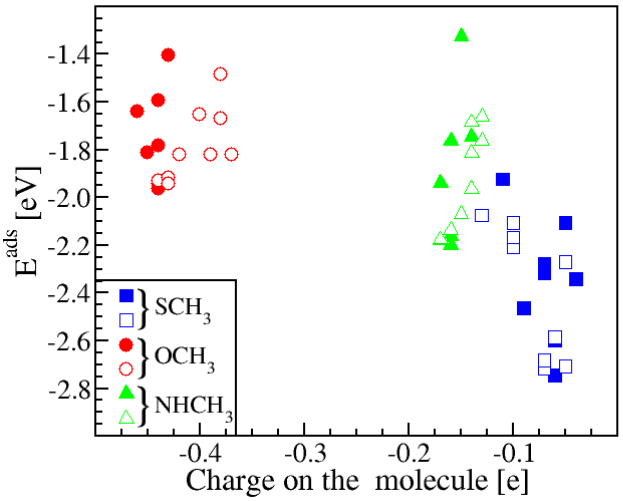

Fig. 5 Adsorption energy E_{ads} (in eV) of SCH_3 (blue), OCH_3 (red) and $NHCH_3$ (green) radicals as a function of the charge on the adsorbed molecule (in e). Adsorptions on flat surfaces are represented by solid symbols and those involving adatoms by empty symbols.

The adsorption energies of OCH_3 on gold are significantly lower than that of SCH_3 but not very far from that of $NHCH_3$ (see Fig. 2). Indeed, the lowest adsorption energies are -2.744 eV for SCH_3, -2.199 eV for $NHCH_3$ and -1.962 eV for OCH_3. Concerning the structure of the adsorbates, $NHCH_3$ and OCH_3 have shorter adsorption equilibrium distances than those of SCH_3, and slightly larger angles of inclination with respect to the surface. There are noticeable similarities between the energetic and structural adsorption characteristics of the methoxy and of the methylamine radicals. However, one can notice a significant difference in the charge transferred from the surface to the adsorbed molecule, which is 3 times larger in the case of the methoxy radical.

Based on the present study, one observes that the adsorption on an adatom is not systematically favoured with respect to that on a flat surface. Indeed, it is sig-

nificantly favoured only in the case of $NHCH_3$ adsorption on Au(111) but, in all other investigated cases, it is either competitive or less favourable than adsorption on the defectless gold surfaces, in which the molecule is generally closer to the surface. At this point, it should be recalled that there is experimental evidence of the existence of dispersion forces acting between a gold surface and a XCH_3 molecule, leading to the tendency of XCH_3 groups to be inclined towards the surface and closer to it. One can cite the studies mentioned in the introduction describing an inclination of the CH_3 group of methylamine towards a gold surface [12] or stipulating that dispersion interactions have to be taken into account to get closer to the experimental data in terms of relative height of the sulfur atom of SCH_3 over a gold surface [19]. The present work highlights the fact that weak interactions may be central in determining the preferential adsorption sites of groups as small as XCH_3.

4 Conclusion

In the present paper, we have compared the structures and adsorption energies of a methoxy radical with those of methanethiol and methylamine radicals, by taking the dispersion forces into account in our DFT simulations. We have studied both adsorption on flat surfaces (Au(111), Au(100) and Au(110)) and on surface defects (adatoms) in order to evaluate the effect on adsorption of the undercoordinated sites. We showed that the adsorption energy of OCH_3 on gold is significantly lower than that of SCH_3 but not very far from that of $NHCH_3$. Regarding the adsorption as a function of the crystallographic facet, we have observed an identical overall trend with adsorption of the same order on Au(110) and Au(100) and less favorable on Au(111). During the structural analysis, we noted that there are strong similarities between the adsorption conformations of the methylamine radical and of the methoxy group. Whatever the molecule, we found that the charge transfer goes from the surface to the molecule, with a much larger charge transferred in the case of OCH_3. The charge transferred to SCH_3 is very small, while that transferred to $NHCH_3$ is slightly larger, but still three times smaller than in the case of methoxy. Concerning the competition between adsorption sites, we observed that undercoordinated atoms are not systematically more favoured than flat surfaces.

Acknowledgements N.T. thanks C. Lacaze-Dufaure for very helpful discussions. This work was granted access to the HPC resources of the CALMIP supercomputing center (Grant p1303) and of the Institute for Development and Resources in Intensive Scientific Computing IDRIS (Grant i2015087375). It was supported by the French Ministry of Higher Education and Research [XF, PhD grant].

Conflict of interest

The authors declare that they have no conflict of interest.

References

1. D. Cabuzu, A. Cirja, R. Pui, A. Grumezescu, Current Topics in Medicinal Chemistry **15**(16), 1605 (2015). DOI https://doi.org/10.2174/1568026615666150414144750
2. D. Pissuwan, C.H. Cortie, S.M. Valenzuela, M.B. Cortie, Trends in Biotechnology **28**(4), 207 (2010). DOI https://doi.org/10.1016/j.tibtech.2009.12.004
3. J.R. Nicol, D. Dixon, J.A. Coulter, Nanomedicine **10**(8), 1315 (2015). DOI 10.2217/nnm.14.219
4. E. Pensa, E. Cortés, G. Corthey, P. Carro, C. Vericat, M.H. Fonticelli, G. Benítez, A.A. Rubert, R.C. Salvarezza, Accounts of Chemical Research **45**(8), 1183 (2012). DOI 10.1021/ar200260p
5. P. Khanna, R. Gokhale, V. Subbarao, A.K. Vishwanath, B. Das, C. Satyanarayana, Materials Chemistry and Physics **92**(1), 229 (2005). DOI https://doi.org/10.1016/j.matchemphys.2005.01.016
6. O. Voznyy, J.J. Dubowski, J.T. Yates, P. Maksymovych, Journal of the American Chemical Society **131**(36), 12989 (2009). DOI 10.1021/ja902629y
7. H. Kondoh, M. Iwasaki, T. Shimada, K. Amemiya, T. Yokoyama, T. Ohta, M. Shimomura, S. Kono, Physical Review Letters **90**(6), 066102 (2003). DOI 10.1103/PhysRevLett.90.066102
8. M. Roper, M. Skegg, C. Fisher, J. Lee, V. Dhanak, D. Woodruff, R.G. Jones, Chemical Physics Letters **389**(1), 87 (2004). DOI https://doi.org/10.1016/j.cplett.2004.02.109
9. P. Maksymovych, D.C. Sorescu, J.T. Yates, The Journal of Physical Chemistry B **110**(42), 21161 (2006). DOI 10.1021/jp0625964
10. P. Maksymovych, O. Voznyy, D.B. Dougherty, D.C. Sorescu, J.T. Yates, Progress in Surface Science **85**(5), 206 (2010). DOI https://doi.org/10.1016/j.progsurf.2010.05.001
11. J.L.C. Fajín, F. Teixeira, J.R.B. Gomes, M.N.D.S. Cordeiro, Theoretical Chemistry Accounts **134**(5), 67 (2015). DOI 10.1007/s00214-015-1666-y
12. T. Luczak, Colloids and Surfaces A: Physicochemical and Engineering Aspects **280**(1), 125 (2006). DOI https://doi.org/10.1016/j.colsurfa.2006.01.045
13. C. Dri, G. Fronzoni, G. Balducci, S. Furlan, M. Stener, Z. Feng, G. Comelli, C. Castellarin-Cudia, D. Cvetko, G. Kladnik, A. Verdini, L. Floreano, A. Cossaro, The Journal of Physical Chemistry C **120**(11), 6104 (2016). DOI 10.1021/acs.jpcc.6b00604
14. K.A. Assiongbon, D. Roy, Surface Science **594**(1), 99 (2005). DOI https://doi.org/10.1016/j.susc.2005.07.015
15. C. Masens, M. Ford, M. Cortie, Surface Science **580**(1), 19 (2005). DOI https://doi.org/10.1016/j.susc.2005.01.047
16. F.P. Cometto, P. Paredes-Olivera, V.A. Macagno, E.M. Patrito, The Journal of Physical Chemistry B **109**(46), 21737 (2005). DOI 10.1021/jp053273v

17. A. Franke, E. Pehlke, Physical Review B **79**(23), 235441 (2009). DOI 10.1103/PhysRevB.79.235441
18. Y. Yourdshahyan, H.K. Zhang, A.M. Rappe, Physical Review B **63**(8), 081405 (2001). DOI 10.1103/PhysRevB.63.081405
19. M.C. Vargas, P. Giannozzi, A. Selloni, G. Scoles, The Journal of Physical Chemistry B **105**(39), 9509 (2001). DOI 10.1021/jp012241e
20. M.C. Vargas, A. Selloni, Revista Mexicana De Fisica **50**, 536 (2004)
21. H. Grönbeck, H. Häkkinen, R.L. Whetten, The Journal of Physical Chemistry C **112**(41), 15940 (2008). DOI 10.1021/jp807196u
22. X. Fan, X. Fang, R. Ran, W.M. Lau, Physica E: Low-dimensional Systems and Nanostructures **59**, 248 (2014). DOI https://doi.org/10.1016/j.physe.2014.01.029
23. E. Torres, P.U. Biedermann, A.T. Blumenau, International Journal of Quantum Chemistry **109**, 3466 (2009). DOI 10.1002/qua.22055
24. M. Askerka, D. Pichugina, N. Kuz'menko, A. Shestakov, The Journal of Physical Chemistry A **116**(29), 7686 (2012). DOI 10.1021/jp303001x
25. M. Yu, N. Bovet, C.J. Satterley, S. Bengió, K.R.J. Lovelock, P.K. Milligan, R.G. Jones, D.P. Woodruff, V. Dhanak, Physical Review Letters **97**(16), 166102 (2006). DOI 10.1103/PhysRevLett.97.166102
26. D. Grumelli, F.L. Maza, K. Kern, R.C. Salvarezza, P. Carro, The Journal of Physical Chemistry C **120**(1), 291 (2016). DOI 10.1021/acs.jpcc.5b09459
27. M. Benoit, N. Tarrat, J. Morillo, Physical Chemistry Chemical Physics **18**, 9112 (2016). DOI 10.1039/C5CP06258F
28. X. Kuang, X. Wang, G. Liu, Applied Surface Science **257**(15), 6546 (2011). DOI https://doi.org/10.1016/j.apsusc.2011.02.075
29. J.A. Larsson, M. Nolan, J.C. Greer, The Journal of Physical Chemistry B **106**(23), 5931 (2002). DOI 10.1021/jp014483k
30. D. Krüger, H. Fuchs, R. Rousseau, D. Marx, M. Parrinello, The Journal of Chemical Physics **115**(10), 4776 (2001). DOI 10.1063/1.1386806
31. H. Barron, L. Fernández-Seivane, X. López-Lozano, physica status solidi (b) **251**(6), 1239 (2014). DOI 10.1002/pssb.201350183
32. R. Liu, W. Shen, J. Zhang, M. Li, Applied Surface Science **254**(18), 5706 (2008). DOI https://doi.org/10.1016/j.apsusc.2008.03.031
33. F. Iori, S. Corni, R. Di Felice, The Journal of Physical Chemistry C **112**(35), 13540 (2008). DOI 10.1021/jp801542s
34. Z. Li, D.S. Kosov, Physical Review B **76**(3), 035415 (2007). DOI 10.1103/PhysRevB.76.035415
35. R.C. Hoft, M.J. Ford, A.M. McDonagh, M.B. Cortie, The Journal of Physical Chemistry C **111**(37), 13886 (2007). DOI 10.1021/jp072494t
36. A.D. Lewoczko, J.J. BelBruno, Physical Chemistry Chemical Physics **15**, 4707 (2013). DOI 10.1039/C3CP44471F
37. H. You, X. Liu, H. Liu, J. Fang, CrystEngComm **18**, 3934 (2016). DOI 10.1039/C6CE00550K
38. G.C. Wang, Y.H. Zhou, J. Nakamura, The Journal of Chemical Physics **122**(4), 044707 (2005). DOI 10.1063/1.1839552
39. A. Hussain, S. Shah, Surface Science **620**(Supplement C), 30 (2014). DOI https://doi.org/10.1016/j.susc.2013.10.010
40. P. Hohenberg, W. Kohn, Physical Review **136**, B864 (1964). DOI 10.1103/PhysRev.136.B864
41. W. Kohn, L.J. Sham, Physical Review **140**, A1133 (1965). DOI 10.1103/PhysRev.140.A1133
42. G. Kresse, J. Hafner, Physical Review B **47**(1), 558 (1993). DOI 10.1103/PhysRevB.47.558
43. G. Kresse, J. Furthmüller, Computational Materials Science **6**(1), 15 (1996). DOI http://dx.doi.org/10.1016/0927-0256(96)00008-0
44. G. Kresse, J. Furthmüller, Physical Review B **54**(16), 11169 (1996). DOI 10.1103/PhysRevB.54.11169
45. P.E. Blöchl, Physical Review B **50**(24), 17953 (1994). DOI 10.1103/PhysRevB.50.17953
46. G. Kresse, D. Joubert, Physical Review B **59**(3), 1758 (1999). DOI 10.1103/PhysRevB.59.1758
47. M. Methfessel, A.T. Paxton, Physical Review B **40**, 3616 (1989). DOI 10.1103/PhysRevB.40.3616
48. G. Henkelman, A. Arnaldsson, H. Jónsson, Computational Materials Science **36**(3), 354 (2006). DOI https://doi.org/10.1016/j.commatsci.2005.04.010
49. E. Sanville, S.D. Kenny, R. Smith, G. Henkelman, Journal of Computational Chemistry **28**(5), 899 (2007). DOI 10.1002/jcc.20575
50. W. Tang, E. Sanville, G. Henkelman, Journal of Physics: Condensed Matter **21**(8), 084204 (2009)
51. N. Tarrat, M. Benoit, M. Giraud, A. Ponchet, M.J. Casanove, Nanoscale **7**, 14515 (2015). DOI 10.1039/C5NR03318G
52. F. Chiter, V.B. Nguyen, N. Tarrat, M. Benoit, H. Tang, C. Lacaze-Dufaure, Materials Research Express **3**(4), 046501 (2016)
53. D.K. Lorenzo, M. Bradley, W. Unterberger, D. Duncan, T. Lerotholi, J. Robinson, D. Woodruff, Surface Science **605**(1), 193 (2011). DOI https://doi.org/10.1016/j.susc.2010.10.019